

# Putative resolution of the EEEE selectivity paradox in L-type $\text{Ca}^{2+}$ and bacterial $\text{Na}^{+}$ biological ion channels

I. Kh. Kaufman<sup>1</sup>, D. G. Luchinsky<sup>1,2</sup>, W. A. Gibby<sup>1</sup>  
P. V .E. McClintock<sup>1</sup>, A. Stefanovska<sup>1</sup> R. S. Eisenberg<sup>3</sup>

<sup>1</sup>Department of Physics, Lancaster University, Lancaster LA1 4YB, UK.

E-mail: i.kaufman@lancaster.ac.uk

E-mail: w.gibby@lancaster.ac.uk

E-mail: p.v.e.mcclintock@lancaster.ac.uk

E-mail: aneta@lancaster.ac.uk

<sup>2</sup>Mission Critical Technologies Inc., 2041 Rosecrans Ave. Suite 225 El Segundo, CA 90245, USA

E-mail: dmitry\_luchinsky@yahoo.com

<sup>3</sup>Department of Molecular Biophysics and Physiology, Rush Medical College, 1750 West Harrison, Chicago, IL 60612, USA.

E-mail: beisenbe@rush.edu

**Abstract.** The highly selective permeation of ions through biological ion channels can be described and explained in terms of fluctuational dynamics under the influence of powerful electrostatic forces. Hence valence selectivity, e.g. between  $\text{Ca}^{2+}$  and  $\text{Na}^{+}$  in calcium and sodium channels, can be described in terms of ionic Coulomb blockade, which gives rise to distinct conduction bands and stop-bands as the fixed charge  $Q_f$  at the selectivity filter of the channel is varied. This picture accounts successfully for a wide range of conduction phenomena in a diversity of ion channels. A disturbing anomaly, however, is that what appears to be the same electrostatic charge and structure (the so-called EEEE motif) seems to select  $\text{Na}^{+}$  conduction in bacterial channels but  $\text{Ca}^{2+}$  conduction in mammalian channels. As a possible resolution of this paradox it is hypothesised that an additional charged protein residue on the permeation path of the mammalian channel increases  $Q_f$  by  $e$ , thereby altering the selectivity from  $\text{Na}^{+}$  to  $\text{Ca}^{2+}$ . Experiments are proposed that will enable the hypothesis to be tested.

PACS numbers: 87.16.Vy, 41.20.Cv, 05.40.-a, 05.30.-d, 87.10.Mn

## 1. Introduction

Biological ion channels [1] are natural nanopores through cellular membranes. They provide for the fast and highly selective permeation of physiologically important ions like  $\text{Na}^+$ ,  $\text{K}^+$  and  $\text{Ca}^{2+}$ . The conduction and selectivity of e.g. voltage-gated  $\text{Ca}^{2+}$  [2] and  $\text{Na}^+$  channels [3] are known to be determined by the ions' fluctuation-driven movements and interactions inside a short, narrow selectivity filter lined with negatively-charged protein residues<sup>‡</sup>. It is known that permeation may sometime involve the correlated motion of more than one ion [4–6]. Mutation studies [3, 7–9] and simulations [10–15] show that the fixed charge  $Q_f$  provided by the residues is a determinant of the channel's conductivity and valence selectivity. Both nanopores [16] and ion channels [17] exhibit the phenomenon of ionic Coulomb blockade, closely analogous to electronic Coulomb blockade in mesoscopic systems [18–20].

Building on earlier work by Zhang et al. [21] on ionic transport in water-filled periodically-charged nanopores, we used Brownian dynamics simulations of permeation in of  $\text{Ca}^{2+}$  channels to reveal the existence of discrete conduction and selectivity bands as functions of  $Q_f$  [22, 23]. These were not only consistent with earlier speculations [19, 24] but were able to explain both the anomalous mole fraction effect (AMFE) [2] and a number of the puzzling mutation-induced transformations of selectivity in  $\text{Ca}^{2+}/\text{Na}^+$  channels. More recently, we generalized the electrostatic analysis of the multi-ion energetics of conduction bands [23] by introducing an ionic Coulomb blockade model of conduction and selectivity in biological ion channels thereby bringing them into the context of mesoscopic phenomena [17, 25].

Although the Coulomb blockade theory [17, 25] seems to provide convincing explanations of a wide range of ion channel phenomena, it appears to be in direct contradiction to the experimental observation that same electrostatic charge and structure (the so-called EEEE motif) at the selectivity filter seems to select  $\text{Na}^+$  conduction in bacterial channels but  $\text{Ca}^{2+}$  conduction in mammalian channels. We will refer to this apparent anomaly as the *EEEE paradox*. The aim of the present paper is to develop an idea introduced by Cheng et al. [26] leading to a plausible resolution of the paradox.

To set the scene, we start by summarising the generic electrostatics and Brownian dynamics model of calcium/sodium channels (Section 2), including a short description of the Coulomb blockade model of permeation (Section 2.2), and a classification of permeation mechanisms (Section 2.3), also commenting on the success of the Coulomb blockade theory in accounting for AMFE. We then point out (Sec. 2.4) that the EEEE paradox appears to cast doubt on the whole Coulomb blockade picture. In Section 3 we propose a way in which the EEEE paradox may be resolved and we also suggest ways in which the corresponding hypothesis can be tested. Finally, we summarise and draw

<sup>‡</sup> The protein residues are amino acids, of which aspartate (D) and glutamate (E) have negatively charged side chains while lysine (K) and arginine (R) have positively charged side chains; we also mention neutral alanine (A), leucine (L), tryptophan (W) and serine (S).

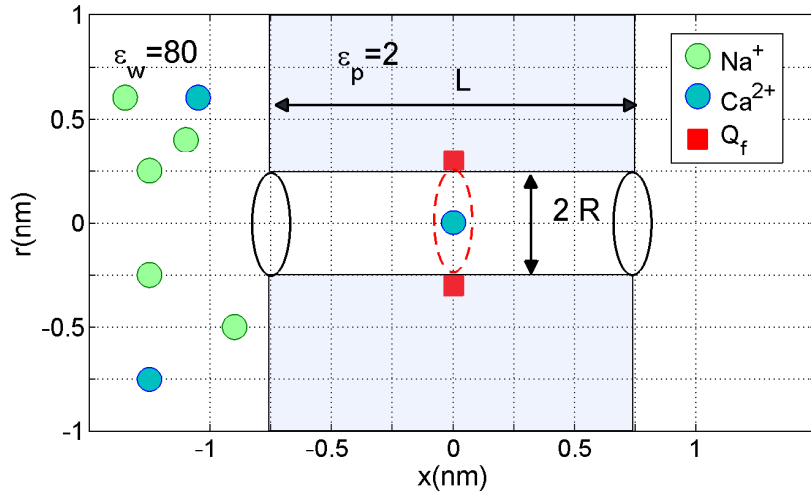


**Figure 1.** Electrostatic model of a  $\text{Ca}^{2+}$  or  $\text{Na}^{+}$  channel, after [22, 23]. Ions move in single file along the channel axis. See text for details.

conclusions in Section 4

In what follows, with SI units,  $e$  is the proton charge,  $z$  the ionic valence,  $\epsilon_0$  the vacuum permittivity,  $T$  the temperature, and  $k_B$  Boltzmann's constant.

## 2. Electrostatic permeation theory

### 2.1. Generic model of calcium channel

The generic electrostatic model of the SF of a  $\text{Ca}^{2+}/\text{Na}^{+}$  ion channel used in earlier electrostatic modelling is shown in Fig. 1. The channel is described as an axisymmetric, water-filled, cylindrical pore of radius  $R = 0.3\text{nm}$  and length  $L = 1.6\text{nm}$  through a protein hub in the cellular membrane. A centrally-placed, uniform, rigid ring of negative charge  $Q_f$  in the range  $0 \leq |Q_f| \leq 7e$  is embedded in the wall at  $R_Q = R$ . The left-hand bath, modeling the extracellular space, contains non-zero concentrations of  $\text{Ca}^{2+}$  and/or  $\text{Na}^{+}$  ions. We take both the water and the protein to be homogeneous continua with relative permittivities  $\epsilon_w = 80$  and  $\epsilon_p = 2$ , respectively, but describe the ions as discrete charges  $q_i = ze$  within the framework of the implicit hydration model moving in single file within the channel, with bulk values of diffusion coefficients  $D_i$ . The BD simulations solve the coupled 3D axisymmetrical Poisson electrostatic equation and 1D overdamped Langevin stochastic equation numerically and self-consistently at each simulation step [5, 10, 22, 23, 27].

Although the model represents a simplification of the actual electrostatics and dynamics of ions and water molecules within the selectivity filter [28], we may note that reduced models can successfully reproduce significant properties of real biological channels [10, 12] and artificial nanopores [16, 21, 28]. Details of the model, its range of validity, and its limitations, have been presented and discussed elsewhere [22, 23].

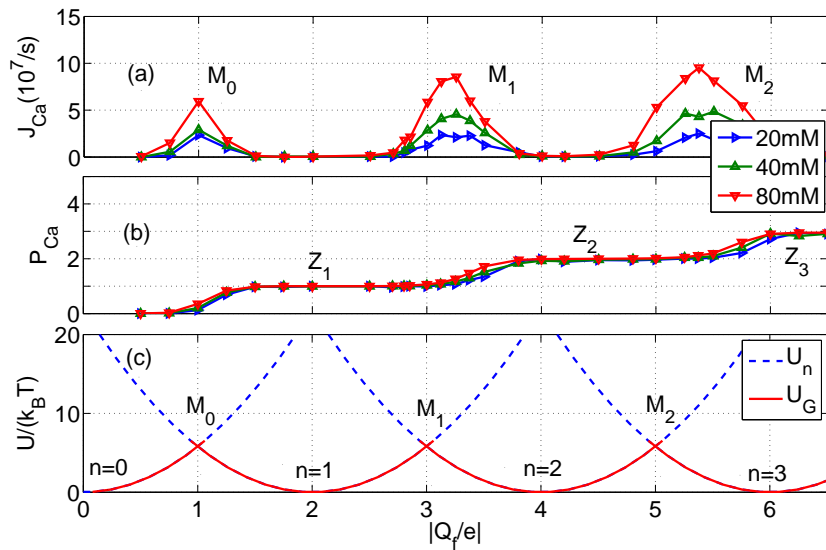


**Figure 2.** Brownian dynamics simulations of multi-ion conduction and occupancy in a  $\text{Ca}^{2+}$  channel model *vs.* the effective fixed charge  $Q_f$ ; (a),(b) are reworked from [22] and (c) from [17]. (a) Plots of the  $\text{Ca}^{2+}$  current  $J$  for pure  $\text{Ca}^{2+}$  baths of different concentration (20, 40 and 80mM as indicated). (b) The occupancy  $P$ . (c) The excess self-energy  $U_n$  and ground state energy  $U_G$  *vs.*  $Q_f$  for channels with  $n = 0, 1, 2$  and 3  $\text{Ca}^{2+}$  ions inside. The conduction bands  $M_n$  and the blockade/neutralisation points  $Z_n$  are discussed in the text.

## 2.2. Coulomb blockade model of ionic permeation

The single- and multi-ion conduction bands found in the BD simulations [22, 23] are shown in Fig. 2(a),(b) which plot the  $\text{Ca}^{2+}$  current  $J$  and channel occupancy  $P$  for pure baths of different concentration. Fig. 2(a) shows narrow conduction bands  $M_0, M_1, M_2$  separated by stop-bands of almost zero-conductance centred on the blockade points  $Z_1, Z_2, Z_3$ . Fig. 2(b) shows that the  $M_n$  peaks in  $J$  correspond to transition regions in channel occupancy, where  $P$  jumps from one integer value to the next, and that the stop-bands correspond to saturated regions with integer  $P = 1, 2, 3, \dots$

Coulomb blockade appears in low-capacitance systems from quantization of the quadratic energy form at a grid of discrete states, provided that the Coulomb energy gap  $\Delta U_n = U_s$  is large enough ( $\Delta U_n \gg k_B T$ ) to block transitions between neighbouring  $\{n\}$  states; that is a strong electrostatic exclusion principle. Fig. 2(c) plots  $U_n$  and the ground state potential energy  $U_G$  as functions of  $Q_f$ . We see a periodic pattern with two kinds of  $U_G$  singular points in, marked as  $M_n$  and  $Z_n$ . The minima of  $U_G$  (and the blockade regions) appear around the neutralisation points  $Z_n = -zen$  where  $Q_G = 0$  and the occupancy  $P_c$  is saturated at an integer value [21, 23]. For divalent  $\text{Ca}^{2+}$  ions  $\Delta U_n \approx 20k_B T$  and hence the blockade is strong. The crossover points  $M_n$  ( $U_n = U_{n+1}$ ) allow barrier-less  $\{n\} \rightleftharpoons \{n+1\}$  transitions; they correspond to the  $P_c$  transition regions and to the conduction peaks in  $J$  [23].

Singular point	Fixed charge	Conduction mode	Conduction event's scheme	Putative identification
<b>M0</b>	1e	Single-ion barrier-less conduction		OmpF porin, NaK channel
<b>Z1</b>	2e	Single-ion Coulomb blockade		
<b>M1</b>	3e	Double-ion knock-on conduction		L-type calcium channel
<b>Z2</b>	4e	Double-ion Coulomb blockade		
<b>M2</b>	5e	Triple-ion knock-on conduction		RyR calcium channel

**Figure 3.** Physical mechanisms of multi-ion blockade and permeation of calcium ions.

The positions of the singular  $Q_f$  points in Fig. 2(c) can be written as:

$$\begin{aligned}
 Z_n &= -zen \pm \delta Z_n \approx 0e, -2e, -4e\dots && \text{(Coulomb blockade)} \\
 M_n &= -ze(n + 1/2) \pm \delta M_n \approx -1e, -3e, -5e\dots && \text{(Resonant conduction)}
 \end{aligned}
 \tag{1}$$

where  $\delta Z_n$ ,  $\delta M_n$  are possible corrections for the singular part of affinity and ion-ion interactions, not accounted for here.

### 2.3. Mechanisms of blockade and permeation

The Coulomb blockade model predicts a very strict and clearly-defined pattern of ionic blockade and conduction [17, 25] where the physical processes occurring at the various conduction and blocking points (see below) are sketched in Fig. 3.

Fig. 4 presents the sequence of singular points that appear for  $\text{Ca}^{2+}$  ions in the generic model as a function of  $Q_f$ , as predicted by (1). The sequence starts from the Coulomb blockade point  $Z_0 = 0e$ , i.e. the neutralized channel is impermeable for divalent ions due to strong Coulomb blockade by the induced charges. This blockade point then repeats itself with period  $\approx 2e$  as  $Z_1$ ,  $Z_2$  etc. with growing number of blocking ions (1 for  $Z_1$ , and 2 for  $Z_2$ ).

The resonant point  $M_0$  shows single-ion resonant (barrier-less) conduction mechanism (see [23] for details) when induced charges balance the charge of the moving ion. The  $M_1$  resonant point represents double-ion blockade combined with double-ion knock-on. In our previous papers we identified  $M_1$  with the L-type calcium channel assuming that protonation might account for the charge discrepancy. We will propose below an alternative explanation in which the L-type channel is actually an

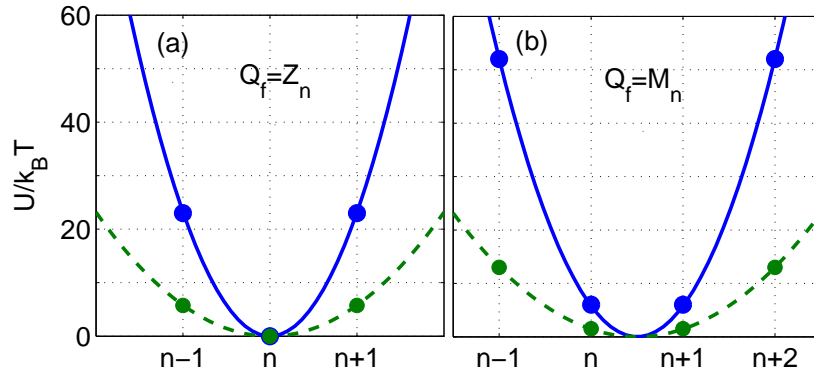


**Figure 4.** Valence-selective Coulomb blockade and resonant conduction. (a) Coulomb blockade. Plots of the self-energy  $U_s$  for  $Z_n$  points vs  $n$ , with  $Ca^{2+}$  (blue),  $Na^+$  (green), and quantization points (filled circles). (b) Resonant conduction. Plots of the self-energy  $U_s$  plots for the  $M_n$  points vs  $n$  with  $Ca^{2+}$  (blue),  $Na^+$  (green), and quantization points (filled circles).

$M_2$  channel. Note that in the absence of a crystal structure for the calcium channel all such explanations are inevitably putative. The  $M_2$  point represents triple-ion blockade combined with triple-ion knock-on. We have already connected this point with RyR calcium channel. The highest resonances are probably related to large-charge mutants of the bacterial sodium channels CaChBac and CavAB [3, 8].

All these mechanisms can be described in terms of single-vacancy conduction [29, 30]. Evenly-charged  $Z_i$  loci provide divalent block while oddly-charged  $M_i$  points provide AMFE, i.e. divalent block plus fast multi-ion barrier-less conduction. In addition, the Coulomb blockade model predicts exponential growth of binding strength with the net charge  $Q_f$ , which agrees well with experiment [17].

Thus the ionic Coulomb blockade model predicts a universal, valence-dependent, periodic pattern of stop/conduction bands similar to the electronic Coulomb blockade oscillations of conductance in quantum dots [18, 20]. It allows us to identify conduction bands with real calcium-conductive channels/mutants. Unlike its electronic counterpart, ionic Coulomb blockade is valence-dependent: the bands  $M_n$  shift in proportion to  $z$  due to (1) and broaden/narrow in proportion to  $z^2$  [31].

Fig. 4(a) plots the energy  $U_n$  of an  $n$ -occupied channel against  $n$  for the blockade/neutralisation points  $Z_n$ . For divalent  $Ca^{2+}$  (full curve)  $U_n$  has a sharp minimum for state  $\{n\}$ , separated from neighbouring  $\{n\pm 1\}$  states by an impermeable barrier of  $20k_B T$ . This is strong blockade closely similar to electronic Coulomb blockade in quantum dots [18, 32]. The same plot for  $Na^+$  ions (dashed curve) reveals a permeable  $5k_B T$  barrier, that is weak ionic Coulomb blockade. Fig. 4(b) show a similar plot for the resonant conduction points  $M_n$ . Again, it is strong ionic Coulomb blockade ( $\Delta U \approx 40k_B T$ ) for  $Ca^{2+}$  ions and weak ionic Coulomb blockade ( $\Delta U \approx 10k_B T$ ) for  $Na^+$  ions.

The ionic Coulomb blockade approach can be also applied to a mixed  $Ca^{2+}$ - $Na^+$

**Table 1.** Alignment of the protein P-loops near the selectivity filters of  $\text{Ca}^{2+}$  [26] and  $\text{Na}^+$  [?] channels. The charged glutamate (E) and aspartate (D) residues that form the electrostatically-active part of the selectivity filter are emboldened. Note that all 4 segments of the NaChBAC selectivity filter are identical. It is not known for sure whether or not the D on p51 of the  $\text{Ca}^{2+}$  channel should be considered as part of the selectivity filter.

Channel	Segment	First residue		
$\text{Ca}_v1.2$	IP	379	p41 L T V F Q C I T M <b>E</b>	p51 G W T D V L Y
	IIP	722	L T V F Q I L T G <b>E</b>	<b>D</b> W N S V M Y
	IIIP	1132	M A L F T V S T F <b>E</b>	G W P E L L Y
	IVP	1432	L L L F R C A T G <b>E</b>	A W Q D I M L
NaChBac			p1 L T L F Q V V T L <b>E</b>	p11 S W A S G V M
	IP - IVP			

bath at the  $Q_f = -3e$  point, which is  $M_1$  for  $\text{Ca}^{2+}$  and  $Z_3$  for  $\text{Na}^+$  ions. The combination  $1\text{Ca}^{2+}+1\text{Na}^+$  (with  $+3e$  charge) inside the SF is neutralized ( $Q_n=0$ ) and so the channel is asymmetrically blocked due to ionic Coulomb blockade (Fig. 4(a)) – which is strong for  $\text{Ca}^{2+}$  and weak for  $\text{Na}^+$ . Similarly  $3\text{Na}^+$  (with  $+3e$ ) also blocks the channel by weak ionic Coulomb blockade at the  $Z_3$  point for  $\text{Na}^+$  ions. Otherwise, a channel contents of  $2\text{Ca}^{2+}$  ( $+4e$ ) gives  $Q_n = +1e$  and resonant conduction (Fig. 4(b)). Hence ionic Coulomb blockade provides a natural explanation of AMFE in  $\text{Ca}^{2+}$  channels consistent with experiment and with analysis in terms of a potential energy landscape [23, 31].

#### 2.4. Apparently anomalous EEEE selectivity in the mammalian $\text{Ca}^{2+}$ channel

Notwithstanding the great success of the Coulomb blockade model in explaining many different, previously puzzling, features of ion channel conduction, the EEEE paradox (see above) represents a serious concern: for the same  $Q_f = -4e$  at the selectivity filter to give rise to both  $\text{Na}^+$  and  $\text{Ca}^{2+}$  resonances is clearly impossible, and therefore the paradox threatens the whole edifice of understanding that has been developed around electrostatics and Coulomb blockade. If we are to retain the Coulomb blockade theory of selectivity, then we are obliged to find an explanation of what we may choose to regard as the anomalous properties of the L-type  $\text{Ca}^{2+}$  channel. We propose such an explanation in Section 3.

### 3. Proposed resolution of the EEEE Paradox in calcium channels

Table 1 describes comparable alignments of the P- and S- segments in  $\text{Ca}_v1.2$  mammalian calcium [?] and NaChBac bacterial sodium [?] channels. It is usually supposed that the selectivity filter of the mammalian calcium channel is based upon a 4-glutamates EEEE locus and hence has a total charge  $Q_f = -4e$ . This locus is

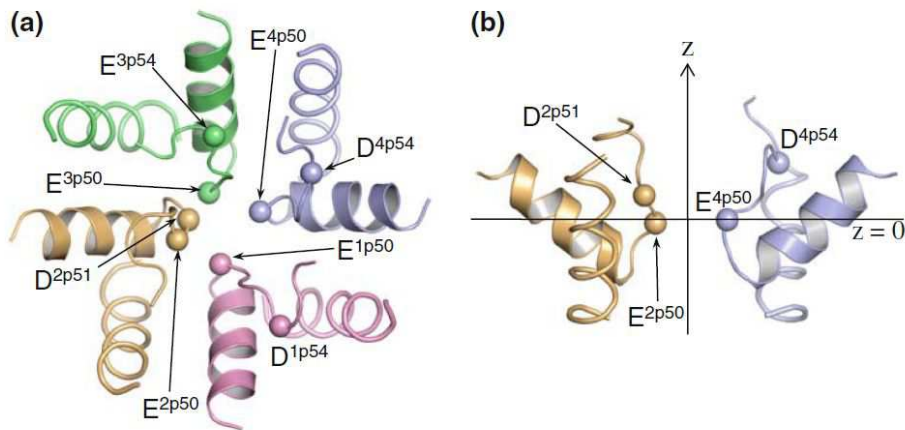


**Figure 5.** The Cav1.2 outer pore model with repeats I, II, III, and IV colored pink, orange, green, and blue, respectively, from [26]. Alpha-carbons of the selectivity filter glutamates  $E^{p50s}$ ,  $D^{2p51}$ , and acid residues in positions p54 are shown as spheres. (a) Extracellular view. (b) Side view with the  $xy$ -plane and the  $z$ -axis.

known to be *highly conserved*, meaning that the sequence has remained the same over many generations despite the vagaries of evolution and speciation, and implying that the structure is important because any small mutation is making the organism less fit. However this proposition not only leads to structural problems [15], but it is also inconsistent with expectations based on the Coulomb blockade model (see above). If we have pseudo-similar loci with similar  $Q_f$  but different function, this directly contradicts our central idea of valence selectivity being of electrostatic origin. Secondly, and in particular, the evenly-charged EEEE locus corresponds to the *blockade point*  $Z_1$  rather than to any of resonant points  $M_i$  (Figs. 2–4). Note that similar EEEE loci in the ChNaBac and NavAB bacterial channels provide for sodium selectivity and divalent block, rather than calcium selectivity.

It always was clear that differences will exist between formally identical loci, and that these differences do not necessarily follow from the structure itself. In the absence of structural data, information related to the positions of particular residues comes mainly from mutagenesis results. One possible source of differences could be protonation [33], which is able to change the effective charge of the selectivity filter, but there is no confirmation from structure simulations, so that this explanation seems speculative and *ad hoc*.

We note, however, that an aspartate  $D^{2p51}$  residue exists in the structure; no associated mutagenesis data are available, so some authors have supposed that it is not located at the selectivity filter [34]. Yet it provides a possible resolution of the EEEE paradox [26]. Repeat II of  $\alpha$ -unit of calcium channel has this  $D^{2p51}$  residue at a position next to the EEEE, and it is highly conserved, so that the locus can be thought as EEEED [26] with nominal charge  $Q_f = -5e$ . Fig. 5 shows the results of Monte-Carlo simulations



of the putative molecular structure by Cheng et al. [26]. The additional D<sup>2p51</sup> aspartate side chain is evidently located very close to the main 4-glutamate EEEE (E<sup>(1-4)p50</sup>) ring both in both the radial (a) and axial (b) directions, and must thus play an equal role in the electrostatic interactions. Following their suggestion [26], we conclude that the calcium channel's locus is actually EEEED, with a charge of  $-5e$ , rather than the EEEE with  $-4e$  which correctly describes the sodium channel.

This would correspond to conduction at the triple-ion M<sub>2</sub> resonant point [17]. Such an identification would differ from our previous conclusion that the L-type channel conducts at the M<sub>1</sub> =  $-3e$  singular point [22, 23], but it appears more likely to be correct. From this viewpoint, there is no EEEE paradox at all, and we are able to include both channels into the Coulomb blockade classification scheme (1).

Finally, we emphasise that both the old and new M<sub>i</sub> identifications for the L-type channel are speculative, and that our tentative conclusions need to be confirmed by mutation studies of the D<sup>2p51</sup> side chain using D→E, D→K and D→A point mutations. We may anticipate that: a D→E mutation giving an EEEEE locus will leave the channel properties unchanged; that a D→A mutation leading to an EEEEA mutant will result in a Na<sup>+</sup>-selective channel exhibiting divalent block similar to the NaChBac channel; whereas the D→K mutation leading to EEEEEK ( $Q_f = -3e \Rightarrow M_1$ ) will yield a new Ca<sup>2+</sup>-selective channel.

#### 4. Conclusions

We have suggested a possible resolution of the EEEE selectivity paradox for calcium/sodium channels, using the Coulomb blockade model to confirm an idea proposed by Cheng et al. [26]. The explanation assumes that the D<sup>2p51</sup> residue is ionized, and that it is on the permeation path and part of the selectivity filter, very close to EEEE ring. Hence the effective locus for calcium channels is actually EEEED implying  $Q_f = -5e$ , providing for a triple-ion knock-on mechanism at the M<sub>2</sub> resonance. This inference awaits experimental confirmation.

#### Acknowledgments

The research was supported by the Engineering and Physical Sciences Research Council UK (grant No. EP/M015831/1). No new data were created during this study.

#### References

- [1] Hille, B., *Ion Channels Of Excitable Membranes* (Sinauer Associates, Sunderland, MA, 2001), 3rd edn.
- [2] Sather, W. A. & McCleskey, E. W., Permeation and selectivity in calcium channels, *Ann. Rev. Physiol.* **65**, 133–159 (2003).
- [3] Tang, L., El-Din, T. M. G., Payandeh, J., Martinez, G. Q., Heard, T. M., Scheuer, T., Zheng, N. & Catterall, W. A., Structural basis for Ca<sup>2+</sup> selectivity of a voltage-gated calcium channel, *Nature* **505**, 56–61 (2014).

- [4] Armstrong, C. M. & Neyton, J., Ion permeation through calcium channels, *Ann. New York. Acad. Sci.* **635**, 18–25 (1991).
- [5] Roux, B., Allen, T., Berneche, S. & Im, W., Theoretical and computational models of biological ion channels, *Quart. Rev. Biophys.* **37**, 15–103 (2004).
- [6] Kharkyanen, V. N., Yesylevskyy, S. O. & Berezetskaya, N. M., Approximation of super-ions for single-file diffusion of multiple ions through narrow pores, *Phys. Rev. E* **82**, 051103 (2010).
- [7] Heinemann, S. H., Teriau, H., Stuhmer, W., Imoto, K. & Numa, S., Calcium-channel characteristics conferred on the sodium-channel by single mutations, *Nature* **356**, 441–443 (1992).
- [8] Yue, L. X., Navarro, B., Ren, D. J., Ramos, A. & Clapham, D. E., The cation selectivity filter of the bacterial sodium channel, NaChBac, *J. Gen. Physiol.* **120**, 845–853 (2002).
- [9] Miedema, H., Meter-Arkema, A., Wierenga, J., Tang, J., Eisenberg, B., Nonner, W., Hektor, H., Gillespie, D. & Meijberg, W., Permeation properties of an engineered bacterial OmpF porin containing the EEEE-locus of  $\text{Ca}^{2+}$  channels, *Biophys. J.* **87**, 3137–3147 (2004).
- [10] Corry, B., Vora, T. & Chung, S. H., Electrostatic basis of valence selectivity in cationic channels, *Biochim. Biophys. Acta-Biomembranes* **1711**, 72–86 (2005).
- [11] Boda, D., Nonner, W., Henderson, D., Eisenberg, B. & Gillespie, D., Volume exclusion in calcium selective channels, *Biophys. J.* **94**, 3486–3496 (2008).
- [12] Boda, D., Monte Carlo simulation of electrolyte solutions in biology: in and out of equilibrium, in D. Gillespie & N. Baker (eds.), *Ann. Rep. Comp. Chem.*, vol. 10 of *Ann. Rep. Comp. Chem.*, chap. 5, 127–164 (Elsevier, 2014).
- [13] Corry, B.,  $\text{Na}^+/\text{Ca}^{2+}$  selectivity in the bacterial voltage-gated sodium channel NavAb, *PeerJ* **1**, e16 (DOI10.7717/peerj.16) (2013).
- [14] Csányi, E., Boda, D., Gillespie, D. & Kristf, T., Current and selectivity in a model sodium channel under physiological conditions: Dynamic Monte Carlo simulations, *Biochim. Biophys. Acta (BBA) – Biomembranes* **1818**, 592–600 (2012).
- [15] Shuba, Y. M., Models of calcium permeation through t-type channels, *Pflügers Archiv-Eur. J. Physiol.* doi: 10.1007/s00424-013-1437-3 (2014).
- [16] Krems, M. & Di Ventra, M., Ionic Coulomb blockade in nanopores, *J. Phys. Condens. Matter* **25**, 065101 (2013).
- [17] Kaufman, I. K., McClintock, P. V. E. & Eisenberg, R. S., Coulomb blockade model of permeation and selectivity in biological ion channels, *New J. Phys.* **17**, 083021 (2015).
- [18] Beenakker, C. W. J., Theory of Coulomb-blockade oscillations in the conductance of a quantum dot, *Phys. Rev. B* **44**, 1646–1656 (1991).
- [19] Stopa, M., Rectifying behavior in Coulomb blockades: charging rectifiers, *Phys. Rev. Lett.* **88**, 146802 (2002).
- [20] Likharev, K. K., SET: Coulomb blockade devices, *Nano et Micro Tech.* **3**, 71–114 (2003).
- [21] Zhang, J., Kamenev, A. & Shklovskii, B. I., Ion exchange phase transitions in water-filled channels with charged walls, *Phys. Rev. E* **73**, 051205 (2006).
- [22] Kaufman, I. K., Luchinsky, D. G., Tindjong, R., McClintock, P. V. E. & Eisenberg, R. S., Multi-ion conduction bands in a simple model of calcium ion channels, *Phys. Biol.* **10**, 026007 (2013).
- [23] Kaufman, I. K., Luchinsky, D. G., Tindjong, R., McClintock, P. V. E. & Eisenberg, R. S., Energetics of discrete selectivity bands and mutation-induced transitions in the calcium-sodium ion channels family, *Phys. Rev. E* **88**, 052712 (2013).
- [24] Eisenberg, R. S., Atomic biology, electrostatics and ionic channels, in R. Elber (ed.), *New Developments in Theoretical Studies of Proteins*, 269–357 (World Scientific, Singapore, 1996).
- [25] Kaufman, I., Gibby, W., Luchinsky, D., McClintock, P. & Eisenberg, R., Coulomb blockade oscillations in biological ion channels, in *Proc. 23rd Intern. Conf. on Noise and Fluctuations (ICNF)*, *Xian*, doi: 10.1109/ICNF.2015.7288558 (IEEE Conf. Proc., 2015).
- [26] Cheng, R. C., Tikhonov, D. B. & Zhorov, B. S., Structural modeling of calcium binding in the selectivity filter of the l-type calcium channel, *Eur. Biophys. J.* **39**, 839–853 (2010).
- [27] Berti, C., Furini, S., Gillespie, D., Boda, D., Eisenberg, R. S., Sangiorgi, E. & Fiegna, C., Three-

- dimensional Brownian dynamics simulator for the study of ion permeation through membrane pores, *J. Chem. Theor. Comp.* dx.doi.org/10.1021/ct4011008 (2014).
- [28] Laio, A. & Torre, V., Physical origin of selectivity in ionic channels of biological membranes, *Biophys. J.* **76**, 129–148 (1999).
- [29] Hille, B. & Schwarz, W., Potassium channels as multi-ion single-file pores, *J. Gen. Physiol.* **72**, 409–442 (1978).
- [30] Schumaker, M. F. & MacKinnon, R., A simple model for multi-ion permeation. Single-vacancy conduction in a simple pore model, *Biophys. J.* **58**, 975–984 (1990).
- [31] Kaufman, I. K., Tindjong, R., Luchinsky, D. G., McClintock, P. V. E. & Eisenberg, R. S., Resonant multi-ion conduction in a simple model of calcium channels, in J. M. Routoure, L. Varani & F. Pascal (eds.), *22nd Intern. Conf. on Noise and Fluctuations (ICNF)*, Montpellier, 24–28 June 2013, doi: 10.1109/ICNF.2013.6578926 (IEEE Conf. Proc., 2013).
- [32] Alhassid, Y., Statistical theory of quantum dots, *Rev. Mod. Phys.* **72**, 895–968 (2000).
- [33] Furini, S., Barbini, P. & Domene, C., Effects of the protonation state of the EEEE motif of a bacterial Na<sup>+</sup>-channel on conduction and pore structure, *Biophys. J.* **106**, 2175–2183 (2014).
- [34] Lipkind, G. M. & Fozzard, H. A., Modeling of the outer vestibule and selectivity filter of the L-type Ca<sup>2+</sup> channel, *Biochemistry* **40**, 6786–6794 (2001).